JOURNAL OF THERMOPHYSICS AND HEAT TRANSFER
Vol. 13, No. 3, July–September 1999

Critical Heat Flux Limits for High Velocity, High Subcooling Water Flows

D. A. Greisen,* D. C. Rousar,† and W. R. Thompson‡
Aerojet, Sacramento, California 95813-6000

Successful design of high heat flux water-cooled systems requires the capability to predict the critical heat flux limits of high velocity, high subcooling water flows. To support this design capability, Aerojet has measured 20 high velocity, high subcooling critical heat flux values and developed a design correlation. The measured critical heat flux values range from 15.2 to 109.7 MW/m^2 (9.3 to 67.1 Btu/in.^{2}-s) with a subcooling range of 54.4–275.2°C (97.9–495.3°F) and a bulk velocity range of 11.6–49.4 m/s (38–162 ft/s). The Aerojet design correlation predicts the measured data to from −17 to +16%. Two predictive techniques from the literature, the Tong correlation (Tong, L. S., "A Phenomenological Study of Critical Heat Flux," American Society of Mechanical Engineers, Paper 75-HT-68, 1968) and the Katto model (Katto, Y., "A Prediction Model of Subcooled Water Flow Boiling CHF for Pressure in the Range of 0.1 to 20 MPa," *International Journal of Heat and Mass Transfer*, Vol. 35, No. 5, 1992, pp. 1115–1123), were evaluated against the 20 critical heat flux conditions presented. The Katto model predicted the current test data more accurately than the Tong correlation. The Katto model predicted the data from −20 to +42%.

Nomenclature

A, B	= correlation constants
C_p	= specific heat
D	= diameter
f	= friction factor
G	= mass flux, kg/(m^2 · s)
h	= forced convection heat transfer coefficient
h_{fg}	= latent heat of vaporization
Ja	= Jacob number
L	= length
P	= pressure
q	= heat flux
$(q/A)_{\text{critical}}$	= critical heat flux
$(q/A)_{\text{sat pool}}$	= saturated pool boiling heat flux
Re	= Reynolds number
T_{bulk}	= fluid bulk temperature
T_{sat}	= saturation temperature
V	= fluid velocity
X	= thermal equilibrium quality
α	= void fraction
β	= correlation factor, Eq. (2)
ΔT_{sub}	= subcooling, $T_{\text{sat}} - T_{\text{bulk}}$
μ	= viscosity
ρ	= density

Subscripts

bulk	= bulk mixed fluid conditions
critical	= critical conditions
ex	= exit conditions
f	= pertains to the liquid in saturated conditions
g	= pertains to the vapor in saturated conditions
meas	= measured condition
pred	= predicted condition
sub	= subcooled condition
W	= wall condition

Presented as Paper 97-2912 at the AIAA/ASME/SAE/ASEE 33rd Joint Propulsion Conference, Seattle, WA, 6–9 July 1997; received 20 July 1998; revision received 8 February 1999; accepted for publication 10 February 1999.

*Engineering Specialist, Mechanical Design, Department 5273, P.O. Box 13222.
†Engineering Product Leader, Department 5270.
‡Engineering Specialist, Heat Transfer Analysis (Retired).

Introduction

MANY high heat flux systems are cooled with water flowing at high velocity and subcooling conditions. While designing these systems it is important to have the capability to predict the critical heat flux (CHF) of water and thereby avoid costly failure. Research investigating the CHF limits of subcooled water flows has been ongoing for many years. This research has involved two tasks: the acquisition of test data and the development of data correlations (or models) capable of predicting the observed data trends. Recent review articles[1–3] present a large amount of the test data available in the open literature and, in addition, provide comparison between these data and many correlations or models that have been proposed. However, some important data on water CHF at high velocity and subcooling conditions were not considered in the recent work because they are unknown to most of the technical community.

The objectives of the current paper are: 1) to present 20 high velocity, high subcooling critical heat flux measurements for water that were not included in the recent review articles, 2) to compare the data with a design correlation for CHF that has been successfully used to design water cooled combustion devices since 1966, and 3) to provide a comparison between the test data and two critical heat flux predictive techniques from the literature.

CHF Test Data

Table 1 presents the tube configurations tested. As shown, the tested tube outside diameters were $\frac{3}{16}$ or $\frac{1}{4}$ in. Wall thicknesses ranged from 0.015 to 0.035 in., whereas the heated L/D ranged from 13.3 to 100. Table 2 presents the flow conditions at the burnout location whereas Table 3 presents the measured CHF and energy balance data. The measured CHFs ranged from 15.2 to 109.7 MW/m^2 (9.3 to 67.1 Btu/in.^{2}-s) whereas the local subcooling ranged from 54.4 to 275.2°C (97.9 to 495.3°F), the local bulk velocity ranged from 11.6 to 49.4 m/s (38 to 162 ft/s), and the local static pressure ranged from 4.64 to 13.79 MPa (673 to 2000 psia). These data were obtained during the performance of contracts AF 04(694)-212 and AF 04(611)-10785 in the 1960s and have been previously published only in contract reports[4,5] that were not widely distributed. Consequently, they were not included in the recent survey work.

The test data were obtained using a nitrogen blowdown type test system with dc electrically heated test sections fabricated from stainless steel and Inconel 718 tubing with circular cross section and uniform wall thickness with the internal diameter ranging from 0.003 to 0.00558 m (0.1175 to 0.22 in.). A typical test system is shown in

Table 1 Tube geometries tested during CHF tests

Test number[a,b]	Tube o.d., in.	Wall thickness, in.	Heated length, in.	Heated L/D	Unheated entrance length, in.
D-115-LC-5	1/4	0.016	2.9	13.3	4.0
D-115-LC-2	3/16	0.035	5.5	47	4.0
D-115-LC-13	1/4	0.035	18.0	100	4.0
D-115-LC-9	3/16	0.016	3.0	19.2	4.0
D-115-LC-6	1/4	0.016	6.1	28.0	4.0
D-115-LC-11	3/16	0.016	2.55	16.4	4.0
D-115-LC-10	1/4	0.016	3.3	15.1	4.0
D-115-LC-7	1/4	0.016	2.9	13.3	4.0
D-115-LC-3	1/4	0.016	6.1	28.0	4.0
D-115-LC-18	1/4	0.016	6.1	28.0	4.0
D-115-LC-16	1/4	0.035	18.0	100.0	4.0
D-115-LC-8	3/16	0.016	3.0	19.2	4.0
D-115-LC-4	3/16	0.016	3.0	19.2	4.0
D-115-LC-17	1/4	0.035	8.1	45.0	4.0
D-115-LC-14	3/16	0.016	2.5	16.0	4.0
D-115-LC-15	3/16	0.016	2.5	16.0	4.0
D-115-LC-19	1/4	0.016	6.1	28.0	4.0
D-115-LC-21	1/4	0.016	6.1	28.0	4.0
HT-4-106	1/4	0.016	4.0	18	5.0
HT-4-105	1/4	0.015	5.0	22.7	5.0

[a]Test series D-115-LC conducted on Contract AF 04(694)-212; test series HT-4 conducted on Contract AF 04(611)-10785.
[b]Tube material for all tests was CRES 347, with the exception of test HT-4-105; tube material for test HT-4-105 was Inconel 718.

Table 2 Flow conditions at burnout location for CHF tests

Test number[a,b]	Static pressure, psia	Flow velocity, ft/s	Bulk temp, °F	Saturation temp, °F	Subcooling ΔT_{sub}, °F
D-115-LC-5	673	52.0	108.7	498.7	390.0
D-115-LC-2	873	44.2	241.8	528.4	286.6
D-115-LC-13	681	43.9	402.0	499.9	97.9
D-115-LC-9	760	108.3	117.2	512.4	395.2
D-115-LC-6	742	111.9	214.4	509.6	295.2
D-115-LC-11	977	141.9	114.0	541.8	427.8
D-115-LC-10	862	147.8	192.3	526.7	334.4
D-115-LC-7	1523	51.8	102.9	598.2	495.3
D-115-LC-3	1550	47.5	156.3	600.6	444.3
D-115-LC-18	1494	54.2	208.9	595.7	386.8
D-115-LC-16	1510	45.6	470.0	597.1	127.1
D-115-LC-8	1494	100.9	121.3	595.7	474.4
D-115-LC-4	1670	95.6	180.2	610.7	430.5
D-115-LC-17	1573	79.1	398.9	602.6	203.7
D-115-LC-14	1286	162.2	105.7	571.7	466.0
D-115-LC-15	1285	139.3	213.0	571.7	358.7
D-115-LC-19	1578	66.2	216.0	603.0	387.0
D-115-LC-21	1557	54.6	247.0	601.2	354.2
HT-4-106	1020	38.0	282.0	547.0	265.0
HT-4-105	2000	48.1	165.0	636.0	471.0

[a]Test series D-115-LC conducted on Contract AF 04(694)-212; test series HT-4 conducted on Contract AF 04(611)-10785.
[b]All tests were conducted with distilled water except: DC-115-LC-19 used Azusa, California, tap water and DC-115-LC-21, HT-4-106, and HT-4-105 used deionized water.

Fig. 1. The burnout, or CHF, was determined by stepwise increasing the test section heat flux until the wall temperature at a point on the test section (almost always near the outlet end) increased suddenly, and test section failure occurred. All thermal and flow conditions were allowed to achieve steady state at each heat flux level. Repeat testing on a subsequent program demonstrated data repeatability within 1% on CHF and 3% on the product of velocity and subcooling.

Sixteen of these CHF measurements were made with distilled water, 3 with deionized water, and 1 with Azusa, California, tap water. In the relatively short-duration CHF tests (3–5 min, typically), the tap water and deionized water results were comparable to the distilled water results. Long-duration tests were also conducted at fixed heat flux levels well below the burnout heat flux with tap water and deionized water. Nothing unusual was observed with deionized water in a 46-min test, but severe wall temperature oscillations occurred in the long-duration tap water test, which were attributed to the formation of scale on the tube i.d. that periodically dislodged. [The tap water conditions were total hardness = 403 ppm (CO_2 and CO_3), conductivity = 686 $\mu\Omega/cm^3$, resistivity = 1460 Ω/cm^3; heat flux: 11.3 Btu/in.^{2}s; wall temperature: 1000–1400°F; and $\frac{1}{4}$ in. o.d. × 0.016 in. wall tube.]

Table 3 Measured CHF conditions

Test number[a]	$(V\Delta T_{sub})/1000$, ft°F/s	Measured CHF, Btu/in.^{2}-s	Burnout point,[b] in.	Energy balance,[c] (%)
D-115-LC-5	20.28	26.7	0.1875	+12.2
D-115-LC-2	12.67	19.3	0.5	+13.4
D-115-LC-13	4.29	9.3	0.1875	+10.1
D-115-LC-9	42.80	40.4	0.125	+1.7
D-115-LC-6	33.03	32.0	0.125	−6.2
D-115-LC-11	60.70	63.2	0.1875	+6.2
D-115-LC-10	49.42	45.2	1.0	+5.4
D-115-LC-7	25.66	27.0	0.25	+8.5
D-115-LC-3	21.10	20.6	0.75	+31.2
D-115-LC-18	20.97	20.0	0.25	+0.8
D-115-LC-16	5.79	9.3	0.125	−14.1
D-115-LC-8	47.87	46.2	0.1875	+9.1
D-115-LC-4	41.16	38.4	0.25	+0.6
D-115-LC-17	16.11	22.5	0.125	——
D-115-LC-14	75.59	67.1	0.1875	+7.1
D-115-LCL-15	49.97	53.6	0.0625	+2.7
D-115-LC-19	25.62	24.5	0.25	——
D-115-LC-21	19.34	21.0	0.1875	——
HT-4-106	10.07	14.6	0.1	+4.7
HT-4-105	22.66	21.5	0.1	——

[a]Test series D-115-LC conducted on Contract AF 04(694)-212; test series HT-4 conducted on Contract AF 04(611)-10785.
[b]Distance from burnout point to downstream end of heated length.
[c]Energy balance = $[(Q_{in} - Q_{out})/Q_{in}] \times 10$.

The uncertainty of the measured CHF data has been characterized by computing the percent difference between the input electrical energy and the measured energy out, indicated by flow rate and bulk temperature measurements:

$$\text{energy balance } \% = \frac{(\text{energy input} - \text{energy out})}{\text{energy input}} \times 100 \qquad (1)$$

These energy balance data are presented in Table 3: 16 of the 20 tests yielded energy balance results, and in 15 of these the balance is within 14%, whereas a single test yielded a 31% energy balance. Thus, the uncertainty of the data is comparable to the accuracy of the data correlation (from −17% to +16%).

Prediction of the CHF

The reliability of a predictive technique is demonstrated by its ability to predict measured test data. Three techniques were compared to the current test data: 1) the Aerojet test data correlation, 2) versions of a correlation initially presented by Tong,[6] and 3) a model presented by Katto.[7] The Tong correlations and Katto model were selected for comparison because they are applicable over the range of conditions evaluated herein, and both techniques have demonstrated ability to predict other CHF data.[3]

Aerojet Test Data Correlation

The Aerojet test data correlation was derived from the 20 CHF measurements presented in Table 3 and has been published previously.[8–10] This design correlation predicts the CHF as a function of local water flow velocity and the local subcooling. The general form of the Aerojet design correlation is

$$(q/A)_{critical} = A + BV\Delta T_{sub} \qquad (2)$$

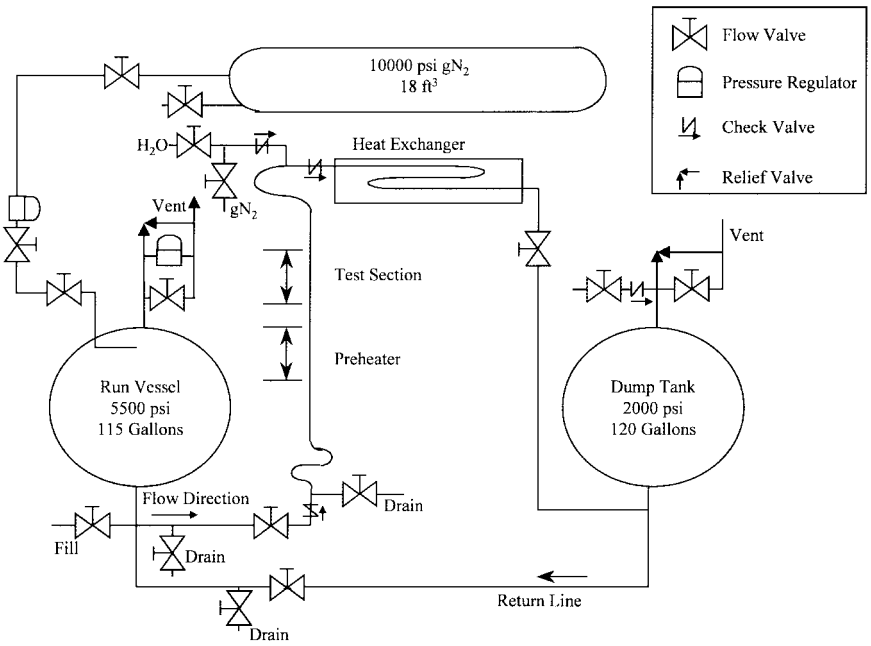

Fig. 1 Simplified schematic of Aerojet CHF test facility.

where A and B are correlating constants, V is the bulk fluid velocity, ΔT_{sub} is the local subcooling ($T_{\text{sat}} - T_{\text{bulk}}$), T_{sat} is the local saturation temperature, and T_{bulk} is the local bulk fluid temperature. During the period 1960–1985, it was found that this simple correlating approach successfully correlated CHF data at high-velocity and subcooling conditions for approximately 40 different fluids. Many of these correlations and the associated data comparisons are presented in Ref. 9.

A theoretical basis for the $V\Delta T_{\text{sub}}$ correlation approach was documented in Ref. 8. It is based on the concept, presented by Levy,[11] that the critical heat flux to a subcooled fluid in forced flow is related to the saturated pool boiling critical heat flux and the forced convection heat flux as

$$(q/A)_{\text{critical}} = (1+\beta)(q/A)_{\text{sat pool}} + h(T_w - T_{\text{bulk}}) \tag{3}$$

where β is a parameter relating heat transfer by bubble agitation and by latent heat content of the bubbles. Equation (3) can be arranged into the Eq. (2) format assuming relatively high subcooling, pressures in the range of 15–80% of the critical pressure, and Reynolds number exponents near 1.0 in the forced convection heat transfer coefficient correlation.[12] This comparison is not totally satisfactory because test data show that the coefficients A and B do not vary with fluid temperature as the analogy between Eqs. (2) and (3) suggests.

The correlation for water CHF was obtained by curve fitting the Table 3 data and is

$$(q/A)_{\text{critical}} = 5.1 + 0.00086V\Delta T_{\text{sub}} \tag{4a}$$

for $4000 < V\Delta T_{\text{sub}} < 76{,}000$ ft°F/s. In Eq. (4a), the units of $(q/A)_{\text{critical}}$ are British thermal units per square inch second and $V\Delta T_{\text{sub}}$ has the units of foot degrees Fahrenheit per second. The following equation presents the water CHF correlation in SI units for the Table 3 data:

$$(q/A)_{\text{critical}} = 8.37 + 0.00256V\Delta T_{\text{sub}} \tag{4b}$$

for $2350 < V\Delta T_{\text{sub}} < 41{,}500$ m°C/s. In Eq. (4b) the units of $(q/A)_{\text{critical}}$ are megawatts per square meter and $V\Delta T_{\text{sub}}$ has the units of meters degrees Celsius per second.

Figure 2a presents the Aerojet design correlation as compared to the measured CHF data. Figure 2b demonstrates that this correlation predicts the measured data to from −17 to +16%.

Reference 8 showed that low $V\Delta T_{\text{sub}}$ data do not agree with Eq. (4); therefore the preceding correlation should not be used for design purposes when $V\Delta T_{\text{sub}}$ is less than 2350 m°C/s (4000 ft°F/s).

Equation (4) has been successfully used to design water-cooled combustion devices operating at high heat fluxes for over 30 years, and no anomalies have ever been observed. Typically, a design point is chosen such that the expected heat flux is about 50% of the predicted CHF.

The most severe test of Eq. (4), as a design correlation, occurred during a calorimeter combustion chamber test reported in Ref. 13. The measured throat region heat flux of 116.6 MW/m^2 (71.8 Btu/in.^{2}s) was much higher than expected. However, the circumferential coolant channel operated successfully even though the measured heat flux was only 17% less than the predicted CHF. [The water flow conditions (outlet) were $V = 64$ m/s (210 ft/s), $T_{\text{bulk}} = 75$°C (168°F), $V\Delta T_{\text{sub}} = 55{,}750$ m°C/s (94,900 ft°F/s) $P =$ 12.3 MPa (1784 psia), and cross section of 0.00178 × 0.00178 m (0.070 × 0.070 in.).]

Tong Correlation

To cover the pressure range of interest, 4.6–13.75 MPa (673–2000 psia), two versions of the Tong correlation were used. A low-pressure version, 0.1–5.0 MPa (14.5–725 psia), was presented in Ref. 3 as the modified Tong. The expression for the modified Tong is

$$\left(\frac{q}{A}\right)_{\text{critical}} = \frac{Gh_{fg}C}{Re^{0.5}} \tag{5}$$

where

$$C = (0.216 + 0.0474P)\Psi$$

$$\Psi = 0.825 + 0.986X_{\text{ex}} \quad \text{if} \quad X_{\text{ex}} > -0.1$$

$$\Psi = 1.0 \quad \text{if} \quad X_{\text{ex}} < -0.1$$

$$\Psi = \frac{1.0}{2 + 30X_{\text{ex}}} \quad \text{if} \quad X_{\text{ex}} > 0$$

The equilibrium quality X_{ex} is evaluated as $(-C_{p,\text{bulk}}) \times (T_{\text{sat}} - T_{\text{bulk}})/h_{fg}$, whereas G is the mass flux.

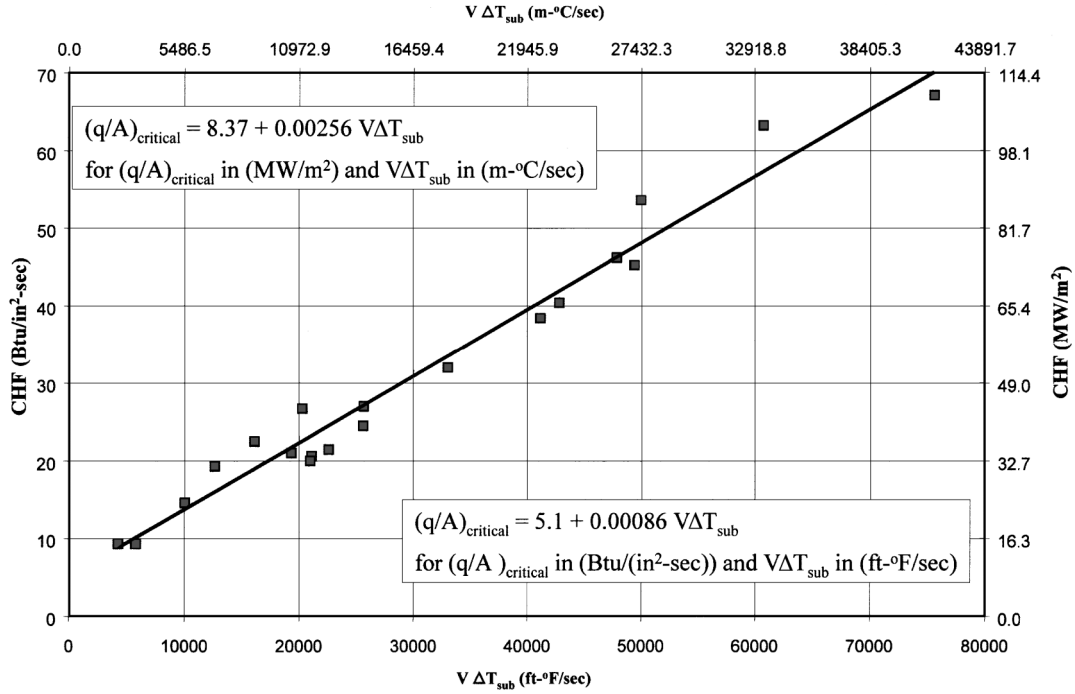

Fig. 2a Aerojet design correlation and test data demonstrates linear nature of predictive approach.

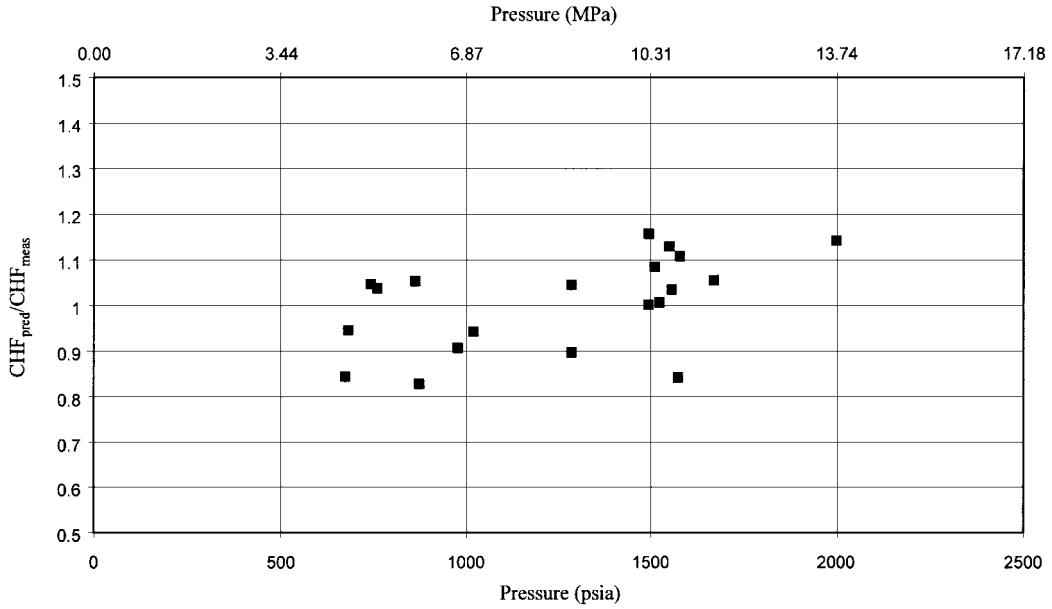

Fig. 2b Aerojet design correlation predicts the measured test data to within from −17 to +16%.

The high-pressure version of the Tong correlation used herein was presented in Refs. 3 and 9 and is referred to the Tong-75 correlation. The recommended pressure range of applicability for this correlation is 7.0–14.0 MPa (1015–2030 psia). The expressions for the Tong-75 correlation are

$$\left(\frac{q}{A}\right)_{\text{critical}} = 0.23 f_0 G h_{fg}\left[1 + 0.00216\left(\frac{P_{\text{ex}}}{P_{\text{crit}}}\right)^{1.8} Re^{0.5} Ja\right] \quad (6)$$

where

$$f_0 = \frac{8(D_e/D_0)^{0.32}}{Re^{0.6}}$$

with $D_0 = 1.27\ (10^{-2})$ m (0.5 in.), and where

$$Re = \frac{GD}{\mu_f(1-\alpha)}$$

with α evaluated per Ref. 14, and where

$$Ja = \frac{C_p(T_{\text{bulk}} - T_{\text{sub}})}{h_{fg}} \frac{\rho_f}{\rho_g}$$

Figure 3 presents a comparison between the measured critical heat flux data and the predicted CHF using the Tong correlations. This comparison illustrates that the modified Tong correlation underpredicted the measured low-pressure [$P < 5$ MPa (725 psia)]

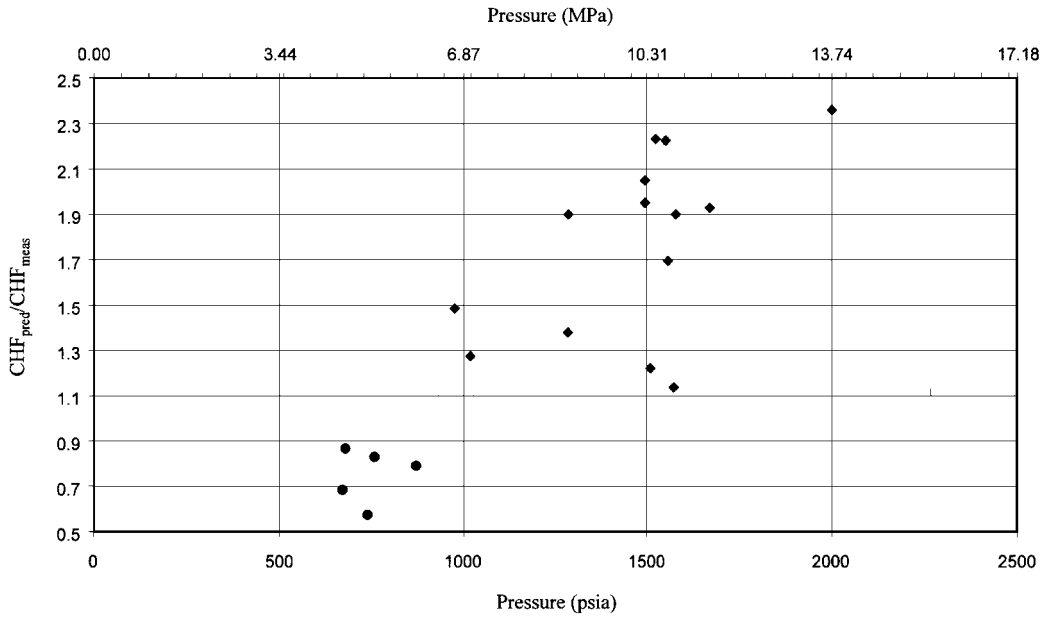

Fig. 3 Comparision of Tong correlation CHF predictions to Aerojet measured CHF test data.

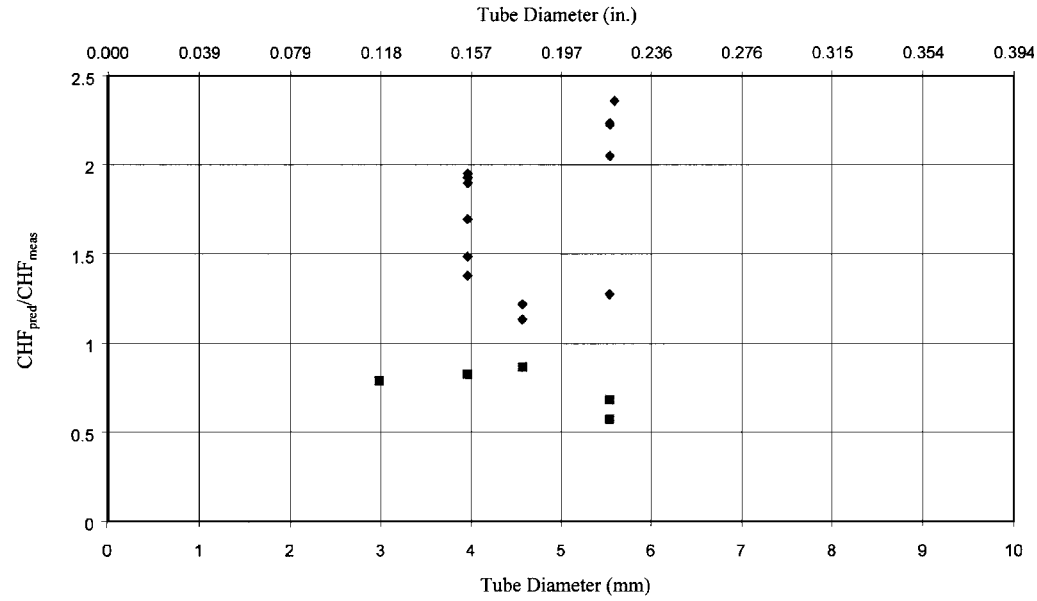

Fig. 4 Effect of tube diameter on the comparison of predicted to measured CHF: ♦, Tong 75, high pressure model; and ■, modified Tong, low pressure.

CHF data whereas the Tong-75 correlation overpredicted the measured high-pressure[$P > 5$ MPa (725 psia)] CHF data. The observed difference between the measured and predicted CHF is similar to that presented in Ref. 3 for the two versions of the Tong correlation used. Figures 4–6 present the ratio of predicted to measured CHF as a function of tube diameter, tube length to diameter ratio, and water mass flux, respectively. Figure 4 presents the effect of tube diameter on the ratio of predicted to measured CHF. For the current test conditions, with tube internal diameters ranging from 3 to 5.588 mm (0.1175 to 0.22 in.), the ratio of predicted to measured CHF ranged from 0.57 to 2.36. This compares, for the same internal diameter range, to approximately from 0.6 to 1.75 from the comparisons of Ref. 3.

Figure 5 presents the effect of tube length to diameter ratio on the ratio of predicted to measured CHF. These data illustrate that as the ratio of the length to diameter is increased beyond 40 the range of predicted to measured CHF is 0.79–1.22, a much better agreement between predicted and measured data than observed for the data with tube length to diameter ratios less than 40. For L/D ratio below 40, the ratio of predicted to measured CHF ranged from 0.57 to 2.36; these data compare to a range of 0.6–1.75 presented in Ref. 3. A conclusion that could be drawn from these limited data comparisons is that as the tube L/D is increased beyond 40 the Tong models predict the measured data within a range of approximately ±20%. The data of Ref. 3 indicates that for $L/D > 40$ most of the test data are predicted with ±25%.

Figure 6 presents the effect of water mass flux on the ratio of predicted to measured CHF. These data illustrate that coolant mass flux does not appear to be a parameter, which explains the observed differences between the predicted and measured CHF.

Katto Model

The Katto model is based on the liquid sublayer dryout mechanism. This model has demonstrated predictive capability for water over a pressure range of 0.1–20 MPa (14.5–2900 psia). In addition, it

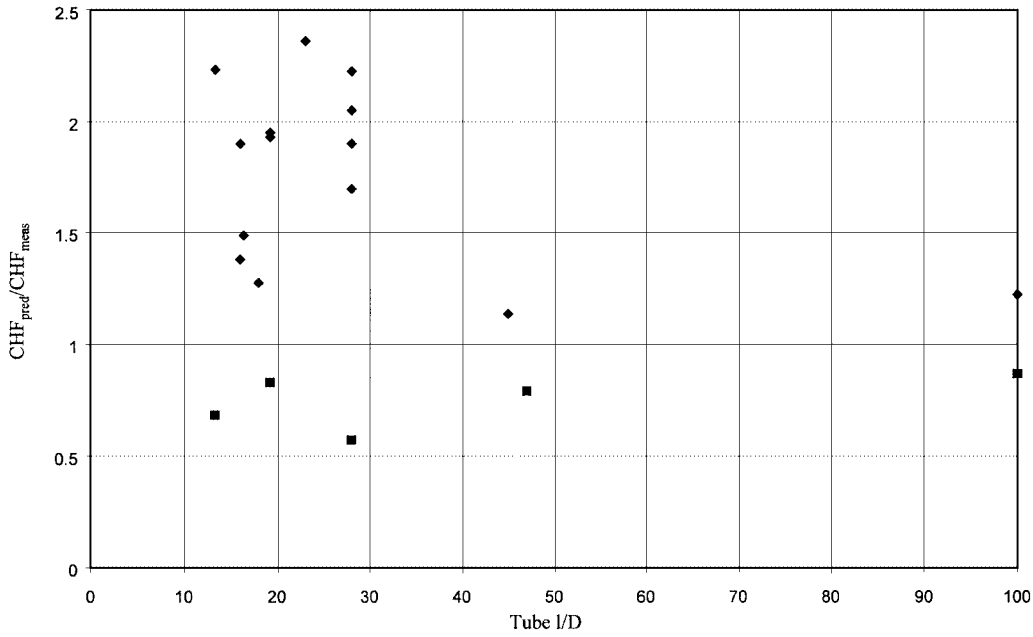

Fig. 5 Effect of tube length to diameter ratio on the comparison of predicted to measured CHF: ♦, Tong 75, high pressure model; and ■, modified Tong, low pressure.

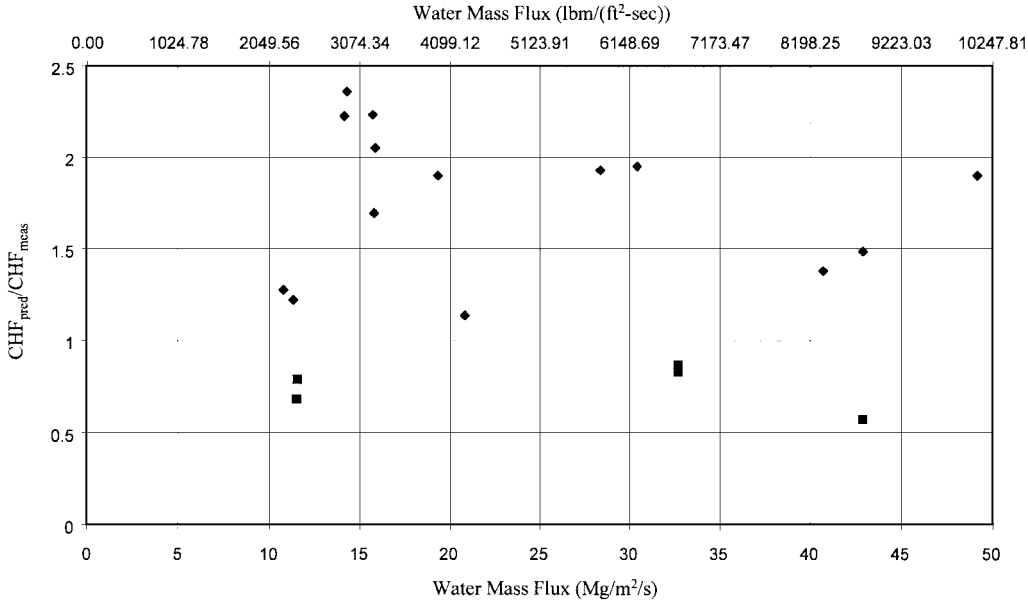

Fig. 6 Effect of water mass flux on the comparison of predicted to measured CHF: ♦, Tong 75, high pressure model; and ■, modified Tong, low pressure.

has been used to predict subcooled flow boiling for nitrogen, helium, and three refrigerants (R-12, R-11, and R-113) (Ref. 15). The predictive procedure for this model is presented in Ref. 7. The premise of the liquid dryout mechanism is that a vapor layer forms between the subcooled core region and a liquid sublayer region along the heated wall, see Fig. 7 (Ref. 15). The CHF is attained when the liquid within the liquid sublayer region vaporizes as a vapor slug passes over. The liquid sublayer vaporization must be completed prior to the passing of the vapor slug, which prevents replenishment of the liquid sublayer with subcooled liquid from the core region.

Review of the literature indicates that care must be taken when using the Katto model. Reference 15 discusses the possibility of obtaining multiple solutions/predictions for the CHF. The correct prediction of the CHF, the one which has physical meaning, is that with the highest value.

Figure 8 presents a comparison between the predicted CHF from the Katto model and the measured CHF data. This favorable

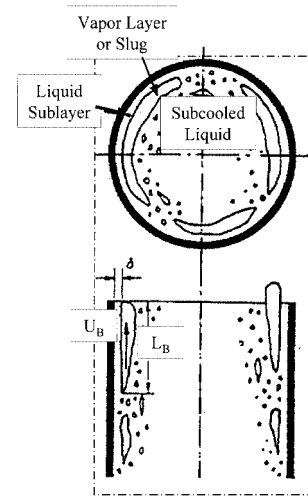

Fig. 7 Basis of Katto model.

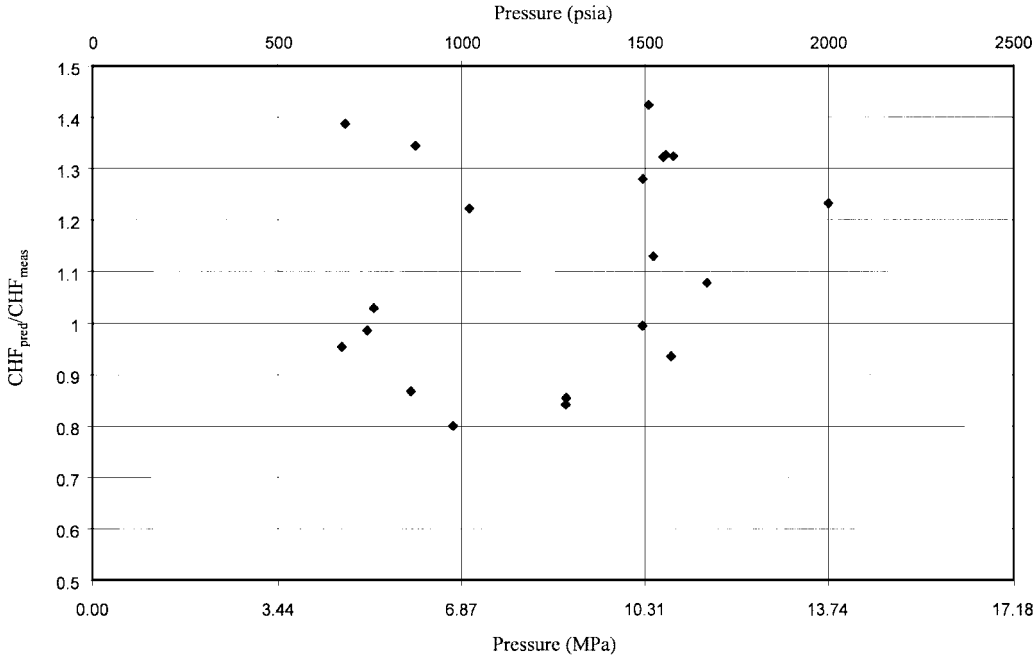

Fig. 8 Katto CHF model predicts the measured CHF test data to from −20 to +42%.

comparison illustrates that the predicted CHF data range from −20 to +42% of the measured CHF data.

Conclusion

There are 20 CHF data points for high velocity, high subcooling water flows presented.

A successful design correlation approach for CHF at high velocity and subcooling is presented. This approach was used to correlate the water CHF test data and the predicted CHF values are within from −17 to +16% of the measured CHF data.

Two predictive techniques selected from the literature were evaluated at the test conditions reported. The Katto model predicted the measured CHFs more closely than the Tong correlations. The Katto model predicted the measured CHF test data within from −20 to +42%. However, application of the Katto model is more rigorous than either the Aerojet or Tong correlations. In addition, because of the iterative solution approach used in the Katto model, caution must be exercised to ensure the correct prediction of the CHF is obtained.

For a rapid evaluation of the CHF for high velocity, high subcooling water flows, the correlation shown on Fig. 2a is recommended for the following range of flow conditions: heat flux, ≤117.4 MW/m ($\leq$71.8 Btu/in.^{2}s); $V\Delta T_{sub}$, 41,500 > $V\Delta T_{sub}$ > 2350 m°C/s (76,000 > $V\Delta T_{sub}$ > 4000 ft°F/s); and pressure, 4.64–13.79 MPa (673–2000 psia).

In the case of flow conditions outside of this range, the Katto model of Ref. 7 is recommended.

Acknowledgments

The contributions of L. E. Dean, N. E. VanHuff, and A. A. McKillop are gratefully acknowledged.

References

[1]Vandervort, C. L., Bergles, A. E., and Jensen, M. K., "The Ultimate Limits of Forced Convective Subcooled Boiling Heat Transfer," Heat Transfer Lab., Dept. of Mechanical Engineering, Aeronautical Engineering and Mechanics, HTL-9, Rensselaer Polytechnic Inst., Troy, NY, May 1992.

[2]Beitel, G. R., "Boiling Heat-Transfer Processes and Their Application in the Cooling of High Heat Flux Devices," Arnold Engineering Development Center, Final Rept. for Oct. 1990–Oct. 1992, AEDC-TR-93-3, Arnold AFB, TN, June 1993.

[3]Celata, G. P., Cumo, M., and Mariani, A., "Assessment of Correlations and Models for the Prediction of CHF in Water Subcooled Flow Boiling," *International Journal of Heat and Mass Transfer*, Vol. 37, No. 2, 1994, pp. 237–255.

[4]Thompson, W. R., and Harkee, J. F., "Burnout Heat Fluxes with Distilled Water at High Velocities and High Degrees of Subcooling," Aerojet, Improved Titan Predevelopment, Contract AF04 (694)-212 Item 5, Final Rept. BSD-TR-65-455-Vol III, Appendix C, Sacramento, CA, Feb. 1966.

[5]Rousar, D. C., and VanHuff, N. E., "Heat Transfer Characteristics of 98%. H_2O_2 at High Pressure and High Velocity," Aerojet, Contract AF04 (611)-10785, Final Rept. AFRPL-TR-66-263, Sacramento, CA, Aug. 1966.

[6]Tong, L. S., "A Phenomenological Study of Critical Heat Flux," American Society of Mechanical Engineers, Paper 75-HT-68, 1968.

[7]Katto, Y., "A Prediction Model of Subcooled Water Flow Boiling CHF for Pressure in the Range of 0.1 to 20 MPa," *International Journal of Heat and Mass Transfer*, Vol. 35, No. 5, 1992, pp. 1115–1123.

[8]Rousar, D. C., "Correlation of Burnout Heat Flux for Fluids at High Velocity and High Subcooling Conditions," M.S. Thesis, Dept. of Mechanical Engineering, Univ. of California, Davis, CA, 1966.

[9]Van Huff, N. E., and Rousar, D. C., "Ultimate Heat Flux Limits of Storable Propellants," *8th Liquid Propulsion Symposium*, Publication 121, Vol. 2, Chemical Propulsion Information Agency, Laurel, MD, Oct. 1966, pp. 227–276.

[10]Rousar, D. C., and Chen, F. F., "Cooling High Pressure Combustion Chambers with Super Critical Pressure Water," AIAA Paper 88-2845, July 1988.

[11]Levy, S., *Critical Heat Flux in Forced Convection Boiling*, Lecture Series on Boiling and Two-Phase Flow for Heat Transfer Engineers, Univ. of California, Berkeley, CA, 1965.

[12]Hines, W. S., "Turbulent Forced Convection Heat Transfer to Liquids at Very High Heat Fluxes and Flowrates," Rocketdyne, Research Rept. 61-14, Canoga Park, CA, Nov. 1961.

[13]LaBotz, R. J., Rousar, D. C., and Valler, H. W., "High Density Fuel Combustion and Cooling Investigation," Final Rept., Contract NAS 3-21030, NASA CR 165177, Sept. 1990.

[14]Thom, J. R. S., Walker, W. W., Fallon, T. A., and Reising, G. F. S., "Boiling in Subcooled Water During Flow Up Heated Tubes of Annuli," *Symposium on Boiling Heat Transfer in Steam Generating Units and Heat Exchanger*, Inst. of Mechanical Engineering, New York, 1965, pp. 226–246.

[15]Katto, Y., "Prediction of Critical Heat Flux of Subcooled Flow Boiling in Round Tubes," *International Journal of Heat and Mass Transfer*, Vol. 33, No. 9, 1990, pp. 1921–1928.